Surface-subsurface model for a dimer-dimer catalytic reaction: a Monte Carlo simulation study



2002 J. Phys. A: Math. Gen. 35 1167

(http://iopscience.iop.org/0305-4470/35/5/304)

INSTITUTE OF PHYSICS PUBLISHING JOURNAL OF PHYSICS A: MATHEMATICAL AND GENERAL

J. Phys. A: Math. Gen. **35** (2002) 1167–1177 PII: S0305-4470(02)27148-6

# Surface–subsurface model for a dimer–dimer catalytic reaction: a Monte Carlo simulation study

**K M Khan**[1,2] **and E V Albano**[2]

[1] Nuclear Physics Division, Pakistan Institute of Nuclear Science and Technology (PINSTECH), PO Nilore, Islamabad, Pakistan
[2] Research Institute of Theoretical and Applied Physical Chemistry (INIFTA), CONICET, UNLP, CIC, Sucursal 4—Casilla de Correo 16, 1900 La Plata, Argentina

Received 19 July 2001, in final form 26 November 2001
Published 25 January 2002
Online at stacks.iop.org/JPhysA/35/1167

**Abstract**

The surface–subsurface model for a dimer–dimer reaction of the type $A_2 + 2B_2 \rightarrow 2AB_2$ has been studied through Monte Carlo simulation via a model based on the lattice gas non-thermal Langmuir–Hinshelwood mechanism, which involves the precursor motion of the $B_2$ molecule. The motion of precursors is considered on the surface as well as in the subsurface. The most interesting feature of this model is that it yields a steady reactive window, which is separated by continuous and discontinuous irreversible phase transitions. The phase diagram is qualitatively similar to the well known Ziff, Gulari and Barshad (ZGB) model. The width of the window depends upon the mobility of precursors. The continuous transition disappears when the mobility of the surface precursors is extended to the third-nearest neighbourhood. The dependence of production rate on partial pressure of $B_2$ dimer is predicted by simple mathematical equations in our model.

PACS numbers: 82.45.Jn, 02.50.Ng, 05.10.Ln, 82.65.+r

## 1. Introduction

Ever since the work of Ziff and his co-workers (Ziff, Gulari and Barshad (ZGB) model) on the catalytic oxidation of CO [1], many efforts have been concentrated on the study of particular models. These models include various systems such as the monomer–monomer [2, 3], monomer–dimer [4–8], monomer–trimer [9, 10], dimer–dimer [11–16], dimer–trimer [10, 17] etc (for a review, see e.g. [18]). All these models are based on the Langmuir–Hinshelwood (LH) mechanism. According to this mechanism the reaction takes place between 'chemisorbed' reactants, i.e. all reactants are adsorbed on the surface and attain thermal equilibrium with the surface before reaction. Therefore the LH mechanism is also called a thermal mechanism. An interesting feature of such models is the occurrence of irreversible phase transitions, which are of first or second order, between poisoned states and a steady reactive state (SRS).

  

The dimer–dimer catalytic reaction $A_2 + 2B_2 \rightarrow 2AB_2$ (having intermediate species AB) has been studied by Albano [11] and Khan *et al* [14] on the surface of a square lattice through computer simulations. The work is based on the LH mechanism. At $y_B = 2/3$ (where $y_B$ is the normalized partial pressure of $B_2$ in the gas phase), the reaction shows a discontinuous transition which separates one poisoned state from another poisoned state. The first poisoned state is a combination of A, AB and isolated vacancies whereas the second poisoned state is a combination of B and isolated vacancies. The diffusion of B atoms does not produce any qualitative difference but if desorption of one dimer is introduced (with probability $P = 1$) the situation changes significantly. The introduction of $B_2$ desorption produces an SRS for $y_B \geqslant 0.70$ until $y_B \approx 1.0$. However, SRS can also be obtained for $P < 1$ as shown by Khan *et al* [14]. This SRS is separated from the poisoned states by two irreversible transitions. The position of the transition points depends upon the value of $P$. The width of the window, which defines the SRS, shows an exponential behaviour with $P$. The observation of Albano [11] for $P = 1$ is, therefore, one extreme case. Maltz and Albano [12] have also shown that an SRS can also be achieved by introducing the AB–AB (OH–OH) reaction in the simple simulation procedure. This reaction step cannot be neglected at low temperatures and even at low $A_2$ (oxygen) coverage in an actual catalytic system [19, 20]. Addition of this reaction step leads to a reactive window with two irreversible phase transitions at $y_B \approx 0.4525$ and 0.6263. However, this situation has been proved controversial as recently Zhonghuti *et al* [13] have shown by means of Monte Carlo (MC) simulation and mean field theory that the AB–AB reaction cannot change the qualitative critical behaviour of the system, i.e. the first-order transition at $y_B = 2/3$.

Many research groups have given evidence that non-thermal processes are also important to understand the catalytic reactions [19–24]. The transient non-thermal mobility caused by the inability to instantaneously dissipate the energy gained by a particle after formation of the surface bond seems to be a common process in nature. Jackson and Persson [24] have studied the dynamics of the 'hot' hydrogen dimer in the Eley–Rideal (ER) mechanism (direct reaction between a gas phase H atom and an adsorbed H atom) using a fully three-dimensional flat surface model for Cu(111). 'Hot' dimers are molecules which after adsorption dissociate, and the remaining 'hot' atoms fly apart up to a maximum distance $R$ from the original adsorption site. Brune *et al* [25] have demonstrated (by means of scanning tunnelling microscopy observations) that oxygen molecules striking the Al(111) surface not only dissociate upon adsorption but also dissipate part of their excess energy in degrees of freedom parallel to the surface. The resulting 'hot' oxygen atoms fly apart, on average, up to a distance of at least 80 Å from the original impingement site, before being accommodated on their respective adsorption sites. After this ballistic flight oxygen atoms remain practically immobile at 300 K. By taking into account this experimental fact, Pereyra and Albano [26] have studied the influence of the 'hot' dimer adsorption mechanism on the kinetics of a monomer–dimer ($CO–O_2$) catalytic reaction. Due to this 'hot' dimer mechanism, they observed a remarkable enhancement of the rate of production (of $CO_2$). The catalytic reaction of $H_2$ and $O_2$ on polycrystalline Pt was studied with quartz crystal micro-beam data in the early work of Harris *et al* [23]. They have analysed the data by means of a mean field approach and have shown that this particular reaction system is an example of a precursor mechanism. Harris and Kasemo [27] have given a detailed discussion on the precursor mechanism of surface reactions. This mechanism involves direct collisions between chemisorbed species and molecules or atoms that are trapped in the neighbourhood of the surface but have not thermalized. The precursor kinetics are generally different from those characteristics of LH or ER mechanisms [19, 23, 24].

Based on the precursor mechanism, Khan *et al* [28] have recently studied the reaction system where movement of the precursors was allowed on the surface only. The subsurface

was considered dead in that study. Remarkably, their model reproduced some experimental results of the real system (i.e. catalytic production of water through dimers $O_2$ ($A_2$) and $H_2$ ($B_2$)). Therefore, they concluded that the model can be taken as a possible model to describe the $H_2$–$O_2$ reaction. There is mounting evidence of the presence of hydrogen in the subsurface [29]. The objective of this work is to explore the effect of the presence of subsurface B atoms on the phase diagram of the dimer–dimer reaction system. This study will be carried out on the surface of a square lattice through MC simulations. In this particular case reaction (collision) of one B atom with chemisorbed species on the surface will be considered up to a maximum distance $R$ having values $d$, $\sqrt{2}d$ and $2d$ ($d$ being the nearest-neighbour distance), respectively, whereas the other B atom will diffuse in the subsurface reservoir. The adsorption of a B atom into the subsurface is not restricted to any particular site. It can be stored within the subsurface reservoir with a restriction that the density of subsurface B atoms (number of B atoms per lattice site) is not greater than unity. If a reacting species (other than B) does not find a B atom from the surface in order to carry out a reaction then a subsurface B atom will be picked with a probability equal to the density of subsurface B atoms. In other words, the proposed model gives preference to surface reaction events in comparison with subsurface–surface reactions.

This paper is structured as follows: in the next section the reaction mechanism and the simulation procedure are discussed. The results are presented and discussed in section 3. Finally the conclusions are inferred in section 4.

## 2. Model and simulation procedure

We may write the equations for the proposed surface–subsurface dimer–dimer model that incorporates the precursor mechanism as follows:

$$A_2(g) + 2S \rightarrow 2A^C \tag{1}$$

$$B_2(g) + S \rightarrow B^P(S) + B^P(SS) + S \tag{2}$$

$$A^C + B^P(S) \rightarrow AB^C \tag{3}$$

$$AB^C + B^P(S) \rightarrow AB_2(g) + S \tag{4}$$

$$A^C + B^P(SS) \rightarrow AB^C \tag{5}$$

$$AB^C + B^P(SS) \rightarrow AB_2(g) + S \tag{6}$$

$$B^P(S) + S \rightarrow B^C \tag{7}$$

$$B^C + A^C \rightarrow AB^C + S \tag{8}$$

$$AB^C + B^C \rightarrow AB_2(g) + 2S. \tag{9}$$

Here (g) indicates the species in the gas phase whereas the precursor and chemisorbed adatoms are represented by $X^P$ and $X^C$, respectively. S represent a vacant surface and $B^P(SS)$ represent the number of B atoms (precursors) diffusing in the subsurface. B atoms (precursors) moving on the surface are represented by $B^P(S)$.

We consider an infinite reservoir filled with $B_2$ and $A_2$ dimers with partial pressures $y_B$ and $1 - y_B$ respectively. We use two layers of a square lattice, so the upper layer is termed surface whereas the lower layer is termed subsurface. We take the lattice size $L = 256$. It is observed that an increase in the lattice size changes the critical pressures slightly but the overall qualitative nature of the phase diagram is not affected [14, 15]. Periodic boundary conditions are used in order to avoid boundary effects.

The simulation starts with a clean surface. If the striking molecule is $A_2$ then it requires two sites to be vacant in order to produce two chemisorbed atoms (equation (1)). If the striking molecule is $B_2$ then it requires only one site to be vacant in order to produce two

precursors (equation (2)). We will assume that one precursor ($B^P(SS)$) diffuses to the subsurface reservoir whereas the second precursor ($B^P(S)$) remains on the surface. If all the subsurface sites are occupied then the diffusion of one precursor to the subsurface will not be possible. In this case a single site present on the surface cannot produce two precursors from the $B_2$ molecule and it will be backscattered. The mobility (and collision with chemisorbed species) of the second precursor $B^P(S)$ is considered for three different cases. In the first case the mobility of the precursor $B^P(S)$ is restricted to the first neighbourhood. Then the mobility of the precursor $B^P(S)$ is extended up to the second- and third-nearest neighbourhood in the other two cases. However, the reaction between two chemisorbed species will be restricted to the first-nearest neighbourhood. The subsurface reservoir containing B atoms will be activated with a probability equal to the subsurface density of B atoms only in the case of unavailability of B atoms from the surface.

In our simulation there are two real variables $y_B$ and the range of surface neighbourhood visited by the precursor ($R$). We have considered three different values of $R$, namely $d, \sqrt{2}d$ and $2d$. The equilibrium coverages are measured as a function of $y_B$. In order to locate the critical points ten independent runs each up to 50 000 MC cycles are carried out. One MC cycle is equal to $L \times L$ trials. If all the ten runs proceed up to 50 000 MC cycles without the lattice becoming poisoned, the particular point is considered to be within the SRS. The poisoning of even a single run is a sufficient criterion for considering the point to belong to the poisoned state. If the run does not end up in a poisoned state, then in order to obtain the coverages corresponding to the SRS the initial 10 000 MC cycles are disregarded (because coverages show large variation in this regime) and averages are taken over the subsequent 40 000 MC cycles (where the variation in the coverages is very small). The values of coverages (production rate) are taken after every ten MC cycles in the regime of 40 000 MC steps, so that the final coverage (production rate) is an average taken over 4000 configurations. The steps involved in the simulation are as follows:

A site is picked randomly. If the site is occupied the trial ends (the molecule is backscattered), else collision of molecules $B_2$ and $A_2$ is considered with probability $y_B$ and $1 - y_B$, respectively. (a) If the colliding molecule is $A_2$ then one of the four neighbouring sites is randomly checked for the presence of another vacancy. The trial ends if no vacancy is found. In the case where a second vacant site is available then step (1) takes place to produce two chemisorbed atoms $A^C$. (b) If the colliding molecule is $B_2$ then after collision with this randomly chosen site two precursors $B^P(S)$ and $B^P(SS)$ are produced via step (2), that move on the surface into the 'environment' of impact of $R$ and in the subsurface reservoir, respectively. We have considered three different ranges of the surface environment: (i) first-nearest neighbourhood ($R = d$), (ii) second-nearest neighbourhood ($R = \sqrt{2}d$) and (iii) third-nearest neighbourhood ($R = 2d$). Each environment consists of a specific pattern for the set of sites around the striking site. For example, the first environment consists of four nearest-neighbouring sites. The second environment contains four nearest- and four second-nearest-neighbouring sites whereas the third environment contains all eight sites of the second environment and four additional third-nearest-neighbouring sites. The simulations of these three environments are carried out separately. (c) The precursor $B^P(S)$ scans all the sites of a particular environment in a random fashion. If any of these sites contains $A^C$ or $AB^C$, reaction step (3) or (4) takes place, which results in the formation of $AB^C$ or $AB_2$ and the precursor ends its life. Here it may be noted that the random choice of $A^C$ or $AB^C$ is made from four sites in the first environment whereas in the second and third environments the random choice of $A^C$ or $AB^C$ is made from eight and 12 sites respectively. It should be pointed out that the randomly chosen reacting species may be $A^C$ or $AB^C$ and hence no priority is given to reaction step (4) over reaction step (3). However, if reaction step (3) or (4) does not take place due

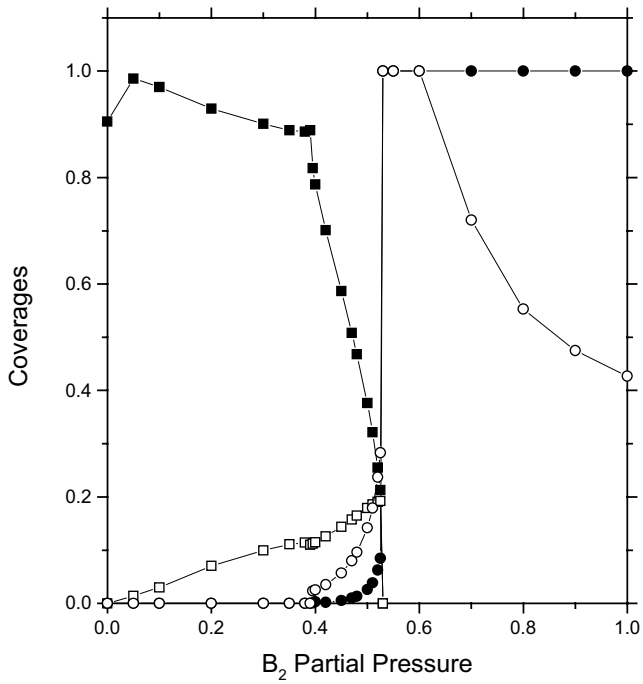


**Figure 1.** Plots of the coverages of $A^C$ (solid square), $B^C$ (solid circle), $B^P(SS)$ (open circle) and $AB^C$ (open square) versus $B_2$ partial pressure for the first environment ($R = d$).

to unavailability of the reacting species and if any of the sites is empty within the particular environment then $B^P(S)$ is chemisorbed on a randomly selected empty site via step (7). This chemisorbed atom scans its four neighbouring sites for the presence of $A^C$ or $AB^C$ in order to complete reaction steps (8) or (9). If $A^C$ is found then $AB^C$ is formed and the site occupied by $B^C$ is vacated. If $AB^C$ is found then $AB_2$ is formed, which desorbs and the sites occupied by $B^C$ and $AB^C$ are vacated. It is worth mentioning that after adsorption of an $A^C$ or the formation of an $AB^C$ radical, it is also necessary to scan their respective nearest neighbourhoods for the presence of $B^C$ in order to complete possible reaction steps (8) and (9). If $B^C$ atoms are not found on the surface then $B^P(SS)$ precursors from the subsurface will be picked with a probability equal to the density of subsurface B atoms in order to complete reaction steps (5) and (6).

## 3. Results and discussion

Figure 1 shows the results corresponding to the first environment ($R = d$), where coverages of the species and production of $AB_2$ are plotted as a function of $y_B$. The values of $y_1$ and $y_2$ are $0.390 \pm 005$ and $0.530 \pm 0.005$, respectively, showing a window width of the order of $\approx 0.14$. For $y_B > y_2$, the surface is poisoned with $B^C$ atoms. However, for $y_B < y_1$, the situation is quite different. In this range the surface is completely covered by a mixture of $A^C$ and $AB^C$. The coverage of $AB^C$ is small whereas that of $A^C$ is large as compared with the dimer–dimer model of Khan *et al* [14]. This is because $B^P$ precusors consume more $AB^C$ and thus create more vacant sites, which are subsequently occupied by $A_2$ molecules due to its high partial pressure. In this range the isolated vacancies are successfully used by $B_2$ molecules. However,

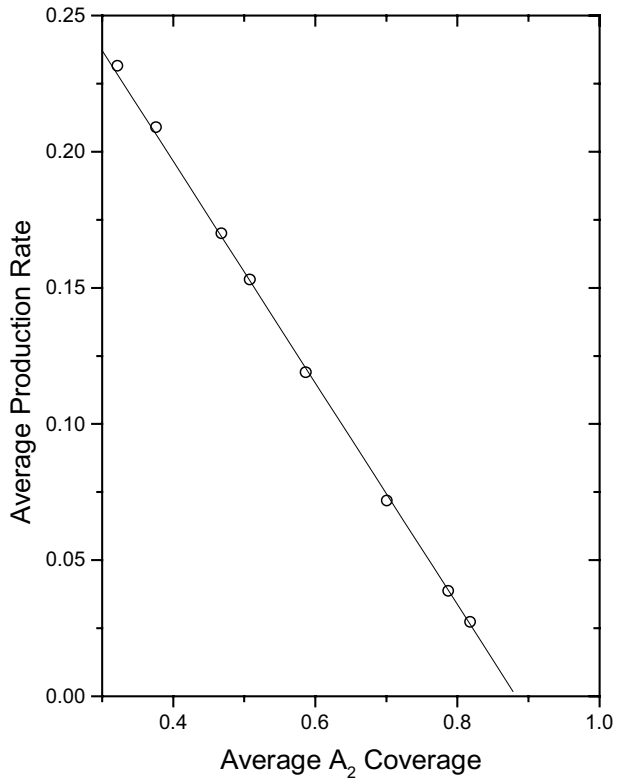


**Figure 2.** Average production rate in the SRS for the case of the first environment ($R = d$) versus average A coverage as obtained after 50 000 MC cycles.

for $y_B > y_2$, the isolated vacancies cannot be successfully used by $B_2$ moloecules because of the unavailability of $A^C$ and $AB^C$ species on the surface. In this region each striking attempt of a $B_2$ molecule results in either chemisorption or backscattering.

The qualitative nature of figure 1 resembles that observed in the ZGB model for CO oxidation despite the fact that the reaction scheme and adsorption rules are different in the two models. In our present model the adsorption of $A_2$ takes place on a pair of nearest-neighbouring sites (like $O_2$ in the ZGB model) whereas adsorption (striking) of $B_2$ molecules takes place on single vacant site. From the created pair of precursors only one precursor is mobile on the surface. At high $A_2$ partial pressure, as the clean surface starts filling with A atoms, the pair of nearest-neighbouring sites will decrease due to occupation of $AB^C$ molecules on single sites. On the other hand, a single vacant site can accommodate a $B_2$ molecule in order to produce two precursors and this single site can be easily available as a result of the $AB^C$–$B^P$ reaction. So, the adsorption of $B_2$ gas will continue until the availability of even a single site (like the ZGB model where the supply of CO will continue until the availability of even a single site). Therefore, this is a case of a pseudo-monomer–dimer type of reaction. This is why the phase diagram as shown in figure 1 is qualitatively very similar to that of the ZGB model and the critical points of the second-order phase transition ($y_1 = 0.390 \pm 005$) and the first-order phase transition ($y_2 = 0.530 \pm 005$) are in agreement with the ZGB model given by 0.387 668 [30] and $0.525 \pm 001$ [1], respectively. It is also interesting to note that the present surface–subsurface model does not change the qualitative picture of the phase diagram

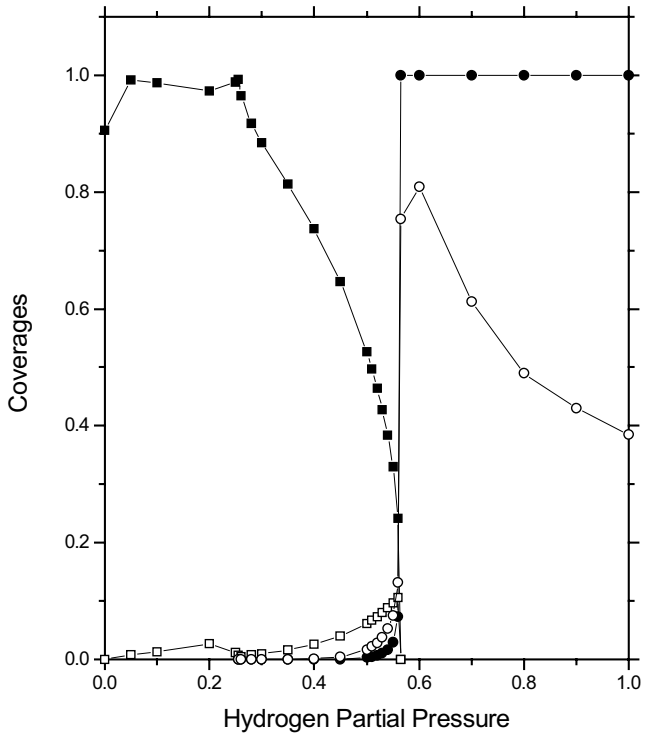


**Figure 3.** The same as in figure 1 but for the second environment ($R = \sqrt{2}d$).

of the system as studied by the surface model of Khan *et al* [28], where both precursors move on the surface up to $R = d$. However, in the present model the width of the window is quite large (≈0.14) as compared with the surface model of Khan *et al* [28] (≈0.08). The position of the second-order transition is the same in the two models. However, in the present model the value of the first-order transition moves towards a higher value of $y_B$. In the surface model the catalytic activity stops at $y_B \approx 0.470$, whereas in the present case picking of $B^P$(SS) from the subsurface reservoir sustains the catalytic activity up to $y_B \approx 0.530$.

Figure 2 shows a plot of the average production rate ($P$) versus the average A coverage ($\theta_A$) within the SRS for a fixed value of the simulation time (50 000 MC cycles). We are only concentrating on the first-environment case ($R = d$). It is observed that when $\theta_A$ decreases, the value of $P$ increases and shows a linear behaviour of the type $P = a - b(\theta_A)$, where $a$ and $b$ are constants that have been evaluated fitting the data shown in figure 2. The obtained values are $a = 0.359 \pm 0.002$ and $b = 0.407 \pm 0.004$, respectively. It should be noted that for $\theta_A \approx 10\%$ of the saturation coverage and high temperature, the experiments show that the reaction rate behaves approximately linearly in $\theta_A$ [31, 32]. In figure 2 $\theta_A$ has a maximum critical value ($\theta_{Max}$) at $\theta_{Max} \approx 0.82$ and a minimum critical value ($\theta_{Min}$) at $\theta_{Min} \approx 0.21$. For $\theta_A > \theta_{Max}$, the catalytic activity is no longer possible due to small adsorption of $B_2$ gas. The catalytic activity can be initiated in this region if we increase the adsorption of $B_2$ gas. We increase this adsorption of $B_2$ gas in the region through increasing the mobility of the precursors into the second- and third-nearest neighbourhood. For $\theta_A < \theta_{Min}$, the catalytic activity again stops due to large adsorption of $B_2$ gas (and less adsorption of $A_2$ gas). The catalytic activity may also be initiated in this region if we adsorb more $A_2$ gas. This condition may be achieved

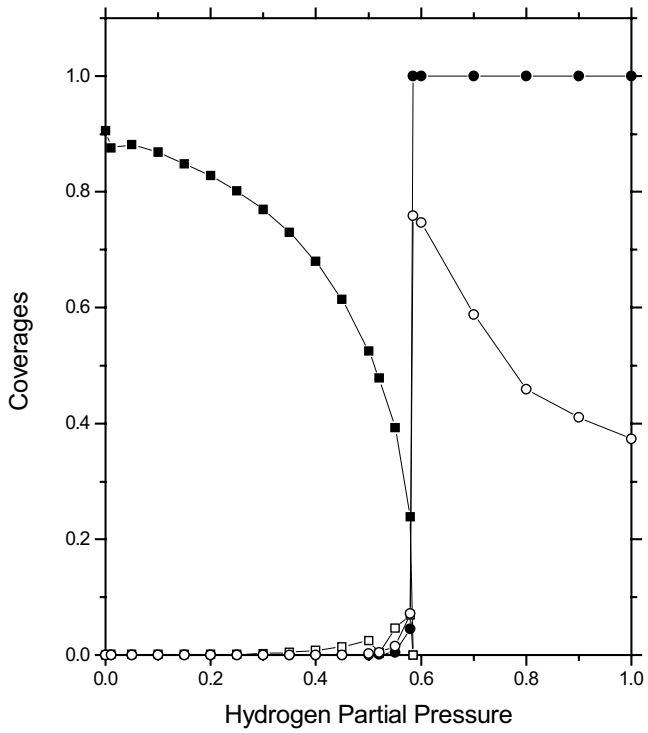


**Figure 4.** The same as in figure 1 but for the third environment ($R = 2d$).

if reaction between chemisorbed and precursor B atoms is considered in our model. In fact, the reaction between $B^P$ and $B^C$ will create more pairs of vacancies and hence the adsorption of $A_2$ gas will be increased. However, in this work this possibility has not been studied.

If the range of the environment of $B^P(S)$ is extended to a higher (e.g. second and third) neighbourhood then it is expected that the positions of $y_1$ and $y_2$ should be changed. In fact, for low pressure of $B_2$ ($y_B < y_1$) the hopping of $B^P(S)$ atoms into the second environment burns more $A_2$ inside the A islands and creates more single vacant sites (due to $AB^C$–$B^P$ reaction). Therefore, indirectly the supply of $B_2$ gas is increased, which will require more $A_2$ to burn and hence $y_1$ should be shifted towards a lower value of $y_B$. In the other extreme case, for high pressure of $B_2$ ($y_B > y_2$) and in the higher environment fewer $B^P$ precursors end their life as $B^C$ atoms (due to the $B^P$ reactivity increase) as compared with the first environment and hence $A_2$ molecules can find more vacant pairs for adsorption. Therefore, $y_2$ should be increased towards higher values of $y_B$. Figure 3 shows the phase diagram for the case when the precursor mobility is increased up to the second environment. This situation is qualitatively similar to that of figure 1 but the values of $y_1$ and $y_2$ are now $0.255 \pm 0.005$ and $0.565 \pm 0.005$, respectively. Thus the reaction window (with a width of the order of $\approx 0.31$) is considerably larger than that in the previous case where the mobility of the precursors was restricted up to the first environment. An interesting situation is observed when the third environment is considered, because here the second-order irreversible transition disappears. The moment $y_B$ is non zero, a continuous production of $AB_2$ starts and at $y_B \approx 0.585$ a first-order irreversible transition stops this catalytic activity. This situation is shown in figure 4.

The dependence of the reaction rate on $y_B$ (or $y_A = 1 - y_B$) cannot be understood from the thermal gas phase kinetics because of the formation of cluster structures which consist of one

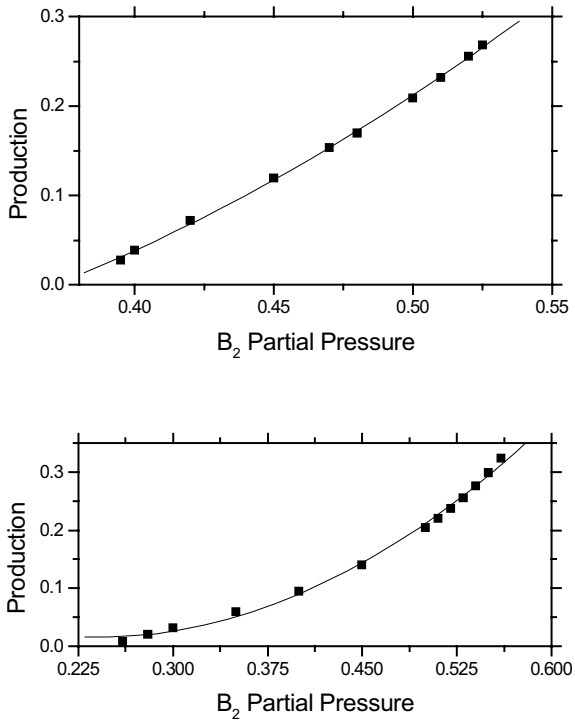


**Figure 5.** Average production rate in the SRS of the first environment (top) and second environment (bottom) versus $B_2$ partial pressure. The fits of the data are also shown.

type of adsorbed molecule. Therefore, the simple prediction of the reaction rate via a lattice gas thermal LH mechanism fails [33]. However, our model can present a simple prediction of the dependence of the reaction rate on $y_B$ for this reaction system. Figure 5 shows the production rate ($P$) of $AB_2$ (within SRS) as a function of $y_B$ for the cases when mobility of the precursors is restricted to the first (top) and extended to the second (bottom) environments. A nice second-degree polynomial fit of the type $P = -0.027 - 1.10\ y_B + 3.157(y_B)^2$ (with standard deviation of the data equal to 0.002 88) satisfies the data of the first environment whereas the data of the second environment are fitted by $P = 0.183 - 1.39\ y_B + 2.896\ (y_B)^2$ (with standard deviation of the data equal to 0.007 29). However, when the mobility of the surface precursor is extended to the third environment, the data are well satisfied by an exponential relation (figure 6) of the type $P = 0.01 \exp(6.239 y_B)$ (with chi squared of the data equal to 0.000 02). The reactivity of $B_2$ dimer in the third environment is higher than that in the second environment, which changes the behaviour of the production rate from polynomial to exponential.

## 4. Conclusions

The precusor mechanism, which assumes that a $B_2$ molecule incident onto a metal site breaks apart and produces two mobile B atoms, one on the surface and the other in the subsurface, incorporates very interesting features in the phase diagram of the dimer–dimer catalytic reaction, which were not seen by considering the LH mechanism only. On the basis of the proposed model, some important aspects of this reaction system can clearly be understood. The model shows a steady reactive region with continuous production of $AB_2$. This reactive

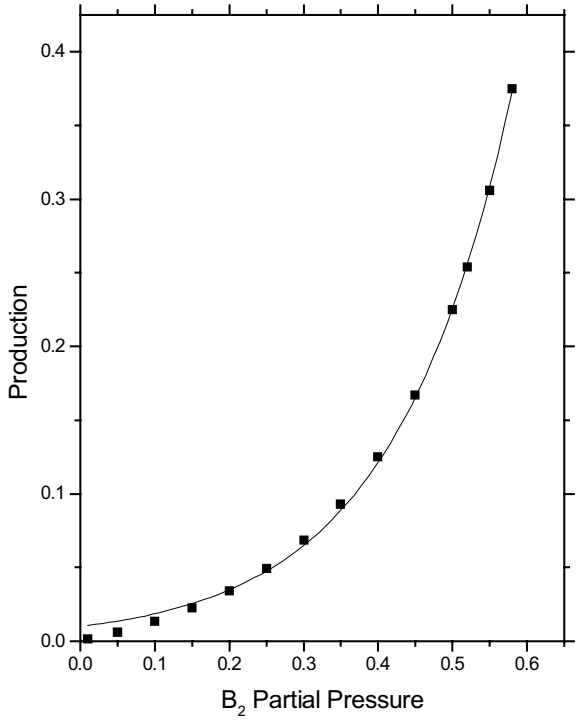


**Figure 6.** Average production rate in the SRS of the third environment versus $B_2$ partial pressure. The fit of the data is shown.

region is limited by continuous and discontinuous irreversible transitions. The phase diagram is qualitatively similar to that of the ZGB model, which shows that our model can lead the behaviour of the usual dimer–dimer reaction to a behaviour like a monomer–dimer reaction. The width of the reactive region increases if the mobility of the precusor is extended to a larger neighbourhood. The continuous transition disappears when the mobility of the precursor is extended up to the third-nearest neighbourhood. Our model can also be taken as a possible model to describe the $H_2$–$O_2$ reaction. Remarkably, some experimentally known facts of the $H_2$–$O_2$ reaction, such as occurrence of a first-order transition [34, 35] and the dependence of the reaction rate on the $A_2$ (oxygen) coverage [31, 32], are also observed in this model. The consideration of movement of one B precursor in the subsurface layer does not change the qualitative picture of the situation when both B precursors move on the surface [28]. However, the quantitative comparison of the present results with those of Khan *et al* [28] shows that due to mobility of one precursor in the subsurface layer the production rate is increased, the window width is widened and the coverage of AB is decreased.

## Acknowledgments

One of the authors (KMK) is deeply indebted to TWAS for an associate membership award. He is also grateful to CONICET for the support of his stay in La Plata. He also acknowledges the kind hospitality of many colleagues during his stay in La Plata, where most of the simulation work was carried out. EVA acknowledges the financial support of CONICET, UNLP and ANPCyT.

## References


[1] Ziff R M, Gulari E and Barshad Y 1986 *Phys. Rev. Lett.* **56** 2553
[2] Sadiq A and Yaldram K 1986 *J. Phys. A: Math. Gen.* **21** L207
[3] Albano E V 1992 *Phys. Rev. Lett.* **69** 656
[4] Yaldram K and Khan M A 1992 *J. Catal.* **136** 279
[5] Khan M A, Yaldram K, Khalil G K and Khan K M 1994 *Phys. Rev.* E **48** 2156
[6] Albano E V 1990 *Surf. Sci.* **235** 351
[7] Albano E V 1992 *Phys. Lett.* A **168** 55
[8] Satulovsky J and Albano E V 1992 *J. Chem. Phys.* **97** 9440
[9] Khan K M, Basit A and Yaldram K 2000 *Surf. Sci.* **469** 65
[10] Khan K M, Basit A and Yaldram K 2000 *J. Phys. A: Math. Gen.* **33** L215
[11] Albano E V 1992 *J. Phys. A: Math. Gen.* **25** 2557
[12] Maltz A and Albano E V 1992 *Surf. Sci.* **277** 414
[13] Zhonghaui H, Lingfa Y and Houwen X 1998 *Phys. Rev.* E **58** 234
[14] Khan K M, Yaldram K, Ahmad N and Qamar-ul-Haque 1999 *Physica* A **268** 89
[15] Khan K M, Yaldram K and Ahmad N 1998 *J. Chem. Phys.* **109** 5054
[16] Yaldram K, Khan K M, Ahmad N and Khan M A 1993 *J. Phys. A: Math. Gen.* **26** 2663
[17] Kohler J and ben-Avraham D 1991 *J. Phys. A: Math. Gen.* **24** L621
[18] Albano E V 1996 *Het. Chem. Rev.* **3** 389
[19] Wolf N O, Burgess D R and Hoffman D K 1980 *Surf. Sci.* **100** 453
[20] Singh-Boparai S P, Bowker M and King D A 1975 *Surf. Sci.* **53** 55
[21] Boato G, Cantini P and Mattera L 1976 *J. Chem. Phys.* **65** 544
[22] Comsa G, David R and Schumacher B J 1980 *Surf. Sci.* **95** L210
[23] Harris J, Kesemo B and Tornqvist E 1981 *Surf. Sci.* **105** L288
[24] Jackson B and Persson M 1995 *J. Chem. Phys.* **103** 6257
[25] Brune H, Wintterlin J, Behm R J and Ertl G 1992 *Phys. Rev. Lett.* **68** 624
[26] Pereyra V D and Albano E V 1993 *Appl. Phys.* A **57** 291
[27] Harris J and Kasemo B 1981 *Surf. Sci.* **105** L281
[28] Khan K M, Albano E V and Monetti R A 2001 *Surf. Sci.* **481** 78
[29] Martins M E, Zinola C F, Andreasen G, Salvarezza R C and Arvia A J 1998 *J. Electroanal. Chem.* **445** 135
[30] Voigt C A and Ziff R M 1997 *Phys. Rev.* E **56** R 6241
[31] Fridell E 1992 *Chem. Phys. Lett.* **188** 487
[32] Fridell E, Elg A P, Rosen A and Kasemo B 1995 *J. Chem. Phys.* **102** 5827
[33] Mai J, Germer T A and Ho W 1989 *Chem. Phys. Lett.* **163** 449
[34] Mai J and von Niessen W 1992 *Chem. Phys.* **165** 65
[35] Germer T A and Ho W 1989 *Chem. Phys. Lett.* **163** 449